Creep load influence on the residual capacity of concrete structure: Experimental investigation

Mirvat Omar, Khalil Haidar, Ahmed Loukili, and Gilles Pijaudier-Cabot

R&DO, Institut de recherches en Génie civil et Mécanique, Ecole Centrale de Nantes,

BP 92101, F-44321 Nantes cedex 3, France

ABSTRACT: Recent experiences and results investigating flexural creep tests with various loading levels are presented. The aim of the study is to analyse the influence of creep on the residual capacity of concrete beams. The load level effects on creep strain are also discussed. Results show that for bending beams subjected to 60% of their load capacity during 40 days, the residual carrying capacity is reduced about 20%. This effect is essentially due to drying creep. Basic creep experiments show that for high load levels there is a coupled effect between creep and damage as tertiary creep is observed. Acoustic emission analyses underline also that damage occurs during creep. These results, which include size effect fracture tests, may serve for the development and the validation of coupled creep-damage models.

Keywords: flexural creep, loading level, residual capacity, acoustic emission

1 INTRODUCTION

In common practice, it is usually assumed that linear visco-elasticity takes place for low load levels and that the instantaneous mechanical behaviour of concrete is elastic. For high load levels, deviation from linearity of the creep behaviour of concrete is expected. Under high sustained loads, cracks grow and interact with visco-elasticity. Some experimental and analytical results concerning non-linear creep can be found in the literature (see among others Bazant, 1988, Gettu and Bazant 1992, Mazzotti and Savoia 2003, Rüsch et al. 1957, Rüsch 1958) but much remains to be learned.

Modelling non linear creep of concrete is of fundamental importance for severely loaded structures as creep may decrease the material strength with increasing time. The evaluation of the residual carrying capacity of structural components is a problem of growing importance for civil engineering structures such as nuclear power plants. Actually, these structures are often exposed to high stresses for a long time, due to what damage develops. Therefore, the results arising from short time tests cannot be considered a sufficient basis for judging the safety of such structures and it is of great interest to devise methods for evaluating their residual capacity.

This problem has drawn the attention of many authors, among them Rüsch and co-workers (1957, 1958), who have carried out the first experiments in order to determine the effect of continuous loading duration on the resistance and deflections of concrete specimens under compression tests. They found that the capacity of a structure subjected to creep loads seems to be 70 to 80% of that observed in short time compression tests.

In the present paper, the main results of a set of experimental creep tests on concrete three points bend specimens at different load levels are presented. The objective is to investigate the ranges of variation of the time response under constant load due to variations of the load level. For each creep test, a different load level has been applied, starting from low levels (36% of peak load) where linear visco-elasticity applies, to high levels (80% of peak load) where tertiary creep causing failure at a finite time can be observed.

Also, this paper deals with the evaluation of the residual capacity of concrete after creep. Concrete B11 used for the construction of the Civaux power plant in France and tested by Granger (1995) is being used in this experimental program.

2 FRACTURE AND CREEP TESTS

Experimental investigation on concrete B11 was performed, involving fracture properties, as well as the visco-elastic behaviour of concrete via creep tests. The experimental program aimed at determining the mechanical characteristics (e.g. tensile strength, compressive strength, fracture energy) of concrete specimens, in order to perform in a next step flexural creep tests on prismatic bending beams.

2.1 *Mix proportions of concrete*

All the specimens were made with a mix which consisted of ordinary Portland cement CPA-CEMII 42.5, fine sand with a maximum size of 5 mm, crushed gravel of size 5 to 25 mm, a superplasticizer a gent (Glenium 21) and water. Mix proportions are shown in table 1. This mixture is characterised by a water-cement ratio of 0.56 and a slump of 4 cm.

Constituents	Concrete B11
	Kg/m^3
Portland cement	350
Gravel G:12.5/25	784
Gravel g:5/12.5	316
Sand	772
Water	195
Superplasticizer	1.3
Mass Density	2360

Table 1. Concrete mixture proportions

2.2 *Fracture tests*

Three different types of tests were performed in order to determine the mechanical characteristics of concrete. Six cylindrical concrete specimens of diameter 16 cm and length 32 cm were used for compressive and splitting tests. The compression tests were performed using 300 KN capacity hydraulic testing machine at a loading rate of 0.5 MPa/s until failure.

The third kind of tests consisted on three points bend size effect experiments on prismatic geometrically similar notched beams. Three different sizes were used, the depths were D1 = 10cm, D2= 20cm, and D3= 40 cm with respective lengths 35, 70, and 140 cm while the thickness was kept constant for all the specimens b = 10 cm. The span to depth ratio was l/D = 3 for all specimens. One notch of depth 0.15D and thickness 3 mm (same for all dimensions) was performed in each specimen by placing a plastic plate at the midpoint perpendicular to the long direction of the mould before casting (Fig. 1). Nine prismatic specimens were cast, three for each size.

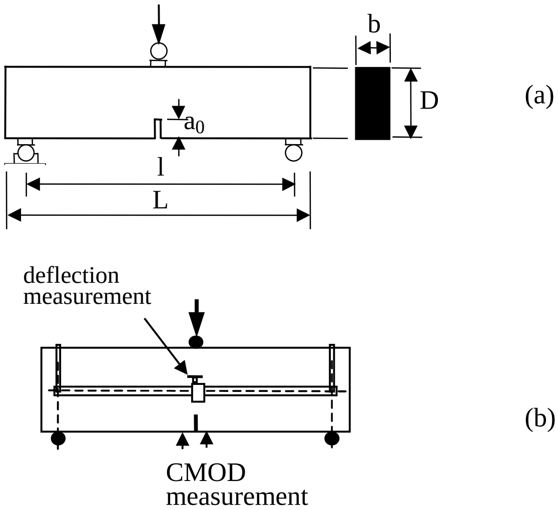

Figure 1. (a) Three point bend experiments on notched specimen; (b) Description of the instrumentation of the mechanical test

Size effect tests followed the guidelines established by RILEM (1990) using a closed – loop testing machine, (160 KN capacity INSTRON machine), under crack mouth opening displacement (CMOD) control. A general view of the experimental set-up is provided in figure 2. Prior to the test, two steel plates with lips to fit into the notch were glued on both sides of the notch. The clip gage used to measure the CMOD was then placed between knife edges attached to the steel plates. In order to measure the deflection of a central point of the beam, a laser extensometer was used. This extensometer was attached at mid - span to a steel beam which was fixed to the concrete beam on two supports at half height and at the ends of it. A metallic plate glued on the specimen at mid span and half height reflect the ray emitted by the laser extensometer and permit to measure the deflection. Deflection was measured in this way so as not to include the effect of local deformations at the support and load points. A data acquisition system was used to record the load, the CMOD, and the deflection with time. Figure 3 shows the average responses for all dimensions. Curing conditions for all specimens were 28 days at 50% RH and controlled temperature of 20° C. Mean values of physical and mechanical properties are summarised in table 2.

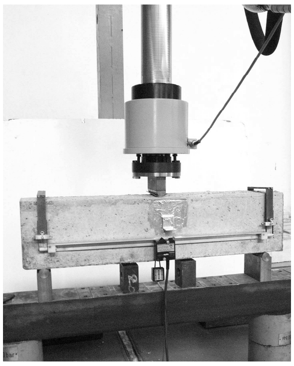

Figure 2. general view of experimental fracture test set-up

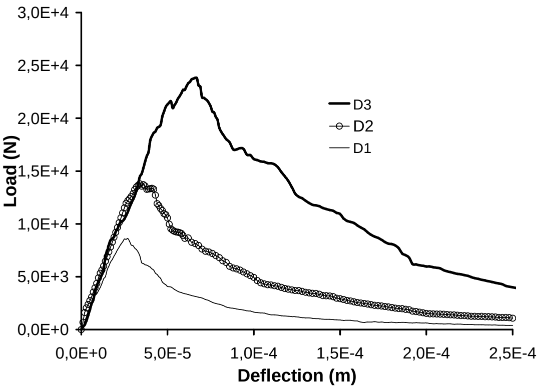

Figure 3. average load-deflection curves for small (D1), medium (D2) and large (D3) sizes

Properties	Mean values
f'_c (MPa)	41.25
f_t (MPa)	3.48
E_{dyn} (MPa)	39000
D1 : F_{max} (daN)	863.42
σ_N (MPa)	5.61
D2 : F_{max} (daN)	1401.13
σ_N (MPa)	4.42
D3 : F_{max} (daN)	2377.31
σ_N (MPa)	4.81
G_f (N/m)	180

Table 2. Physical and mechanical properties of concrete

Another set of three points bending tests was carried out on beams of size D2:10x20x70 cm without notches. These tests were aimed at determining the maximum load of unotched beams in order to calibrate the applied load in the creep tests, where beams having the same geometry have been used. The average maximum load determined from flexural tests on three specimens is about 2409 daN.

2.3 *Creep tests*

The creep tests were performed on frames designed at R&DO. The aim is to load concrete flexural beams with a constant force. The frames have a capacity ranging from 5 to 50 KN and can accommodate geometrically similar specimens of three different sizes. The load is applied by gravity with a weight and counter-weight system which enables a fine tuning of the load. Figure 4 shows a general view of these creep frames.

Figure 4. general view of creep frames

The specimens tested have the same thickness of 10 cm. The smallest D1 is 10 cm high and 35 cm long. The medium D2 is 20 cm high and 70 cm long and the largest D3 is 40 cm high and 140 cm long. Two kinds of creep tests have been performed. The first one is intended to study the influence of the load level on creep. In the second kind of test (which is still in progress), the interaction between creep and fracture of concrete is considered via the associated size effect in structures and the decrease of the fracture energy due to creep. The applied loads in the creep tests have been determined from the previous fracture tests on the same material and the same geometry.

2.3.1 *Load level tests*

It is expected that visco-elasticity and crack growth interaction is related to the solicitation level. Thus, under high sustained loads, damage occurs and the role of microcracking on creep evolution is exhibited. It has also been verified that creep in compression is significantly affected by the applied load amplitude. The greater the load level, the larger the creep strain magnitude.

Twelve prismatic beams were used. For each creep test, a different load level has been applied, starting from low levels to very high levels. The applied loads are given in table 3.

Applied load	notched beams D1	D2	unotched beams D2
	daN	daN	daN
36% F_{peak}	313	-	-
50% F_{peak}	-	-	1198
60% F_{peak}	510	746	1444
70% F_{peak}	-	-	1678
80% F_{peak}	672	1033	1940

Table 3. Applied loads in creep tests

The first set consists of 4 unotched beams of dimension D2 loaded at 50%, 60%, 70% and 80% of the maximum load. These tests are performed at 20°C and 50% RH and the specimens are not protected. Therefore, basic creep and drying creep occur at the same time. The age of concrete at the beginning of the creep tests is 28 days. Figure 5 presents the total displacement (creep displacement plus instantaneous displacement) measured on the specimens versus time for the first three loading levels. These curves indicate that for all loading levels creep kinetics are comparable, with the exception of the specimen loaded at 70% from peak load, where failure due to tertiary creep occurs after 8 days. In this test, we observed an important acceleration of the creep kinetic and then failure. Concerning the specimen loaded at 80% from peak load, total failure occured 2 minutes after applying the load.

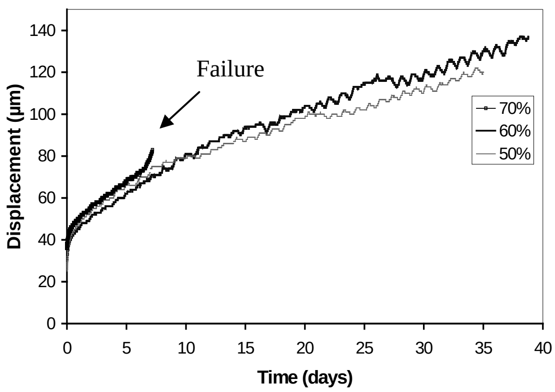

Figure 5. Deflection of unotched beams D2 for different load levels

The second test series consists of two notched beams of dimension D1 loaded at 60 % and 36 % of the maximum load and one notched beam of dimension D2 loaded at 60% of the maximum load. These tests were followed by a third set consisting of two notched beams of dimension D2 and three notched beams of dimension D1 loaded at 80% of the peak load, one of these beams failed after 4 days from loading. Results obtained for this test are not reported here.

Specimens in the second and third test series were protected from desiccation by a double layer of self-adhesive aluminium paper. Hence basic creep was considered only. The experimental measurement of basic creep of concrete requires also that drying shrinkage be prevented. The curing conditions (3 months at 100% RH and 20°C) guaranteed to avoid early age autogeneous shrinkage so that basic creep could be measured only. The basic creep displacement was determined by subtracting the instantaneous elastic displacement from the total displacement.

Figure 6 compare the displacements due to basic creep for the smaller specimens (size D1). It shows the influence of the load level on the basis creep evolution versus the elapsed time.

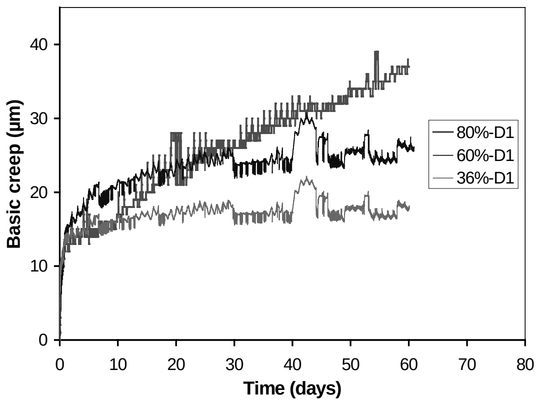

Figure 6. Basic creep displacement of notched beams D1 for 36% , 60% , and 80% of peak load

As expected, increasing the applied load increases the basic creep magnitude. Moreover, creep develops very fast in the first days of loading and stabilises after a few weeks for the two lower loading levels. The specimens loaded at 36% and 60% of the maximum load were cast from the same batch. The results show a variation of the amplitude of basic creep of the 36% and 60% loaded specimens, which increases and decreases again between 40 days and 50 days of loading. This variation is due to a temperature regulation problem, which occurred on the climate control system and which lead to this elevation in the magnitude of deflections measured on loaded specimens. The specimen loaded at 80% is part of the third set of creep tests. It was made from another batch and loaded at a different time but followed the same curing conditions. For this specimen, basic creep increases rapidly. Figure 7 shows the creep test results for the beams of size D2. These plots exhibit the same trend as those in Fig. 6.

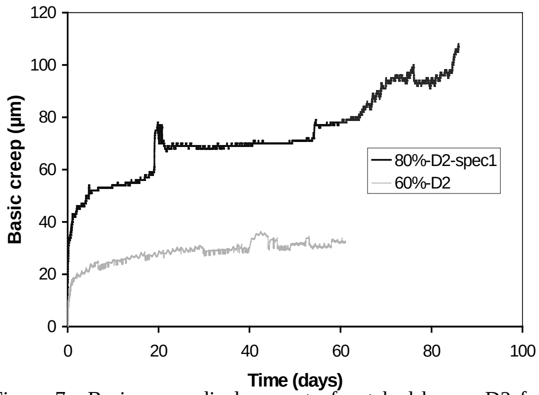

Figure 7. Basic creep displacement of notched beams D2 for 60% , and 80% of peak load

Figure 8 presents a comparison between basic creep displacements obtained on two specimens of size D1 and D2, both of them loaded at 60% from their corresponding maximum load. These results show that the basic creep kinetic for dimension D2 is greater than that of dimension D1.

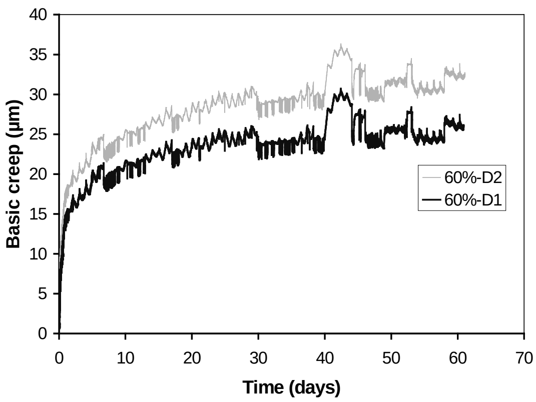

Figure 8. Basic creep displacement of notched beams D1 and D2 loaded at 60% of peak load

This difference is more obvious in the case of a 80% loading level as seen in figure 9. On this plot, we show also the results obtained for the two specimens of each size subjected to the same creep load. The reproducibility of the test is quite satisfactory.

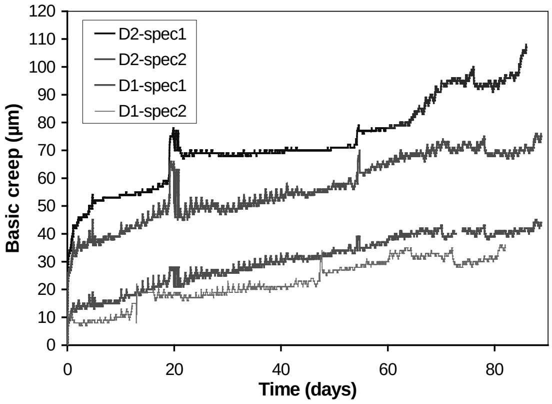

Figure 9. Basic creep displacement of notched beams D1 and D2 loaded at 80% of peak load

2.4 *Acoustic Emission in basic creep tests*

Acoustic emission (AE) occurs when there is a sudden change in energy or energy release, due to flaws and defects nucleation or propagation in a specimen. Most studies have focused on relating acoustic emission characteristics to the properties of the fracture process zone (Maji and Shah 1988), and using AE source location analysis to evaluate damage localisation (Berthelot et al. 1987). We applied this technique to the creep tests presented above.

The AE system used was comprised of an eight-channel MISTRAS system manufactured by Physical Acoustic Corporation. Piezoelectric transducers (R15/C, resonant frequency of 150 KHz) were used. Transducers were placed around the expected location of the process zone, on one side of the specimen, and in a linear array (Fig. 10).

In the present study, the primary aim is to correlate the basic creep evolution and the total number of acoustic events. In other terms, this study is intended to clarify the qualitative relationship between basic creep strain and damage occurring inside the material. More accurate analyses might be performed which include acoustic event localisation in order to visualise the locations of damage. Such tests which require a large number of transducers placed on the same beam will be performed in future experiments.

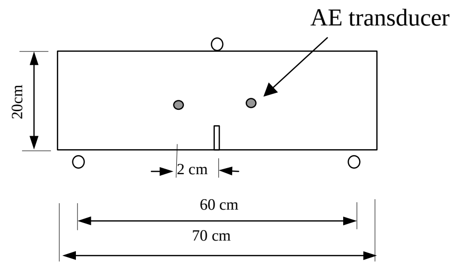

Figure 10. Specimen geometry and AE transducers position

Figure 11 presents the total number of acoustic events versus time and figure 12 shows the corresponding basic creep evolution occurring at the same time.

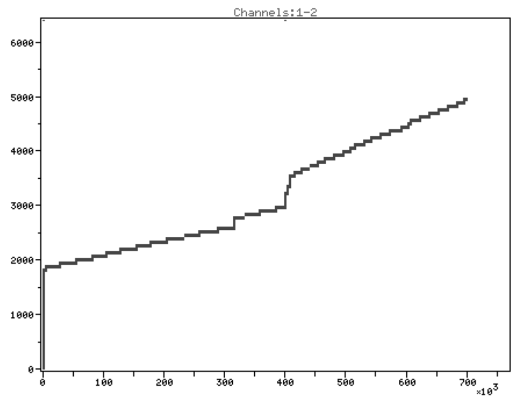

Figure 11. Total number of AE versus time for the 80% basic creep loaded specimen D2

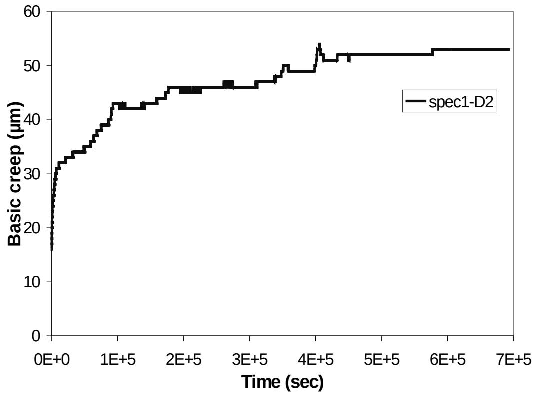

Figure 12. Deflection due to basic creep of a 80% loaded specimen D2

We may observe that the number of AE events increases as basic creep develops. The evolution of the AE number is almost linear. There is a change of slope of the curve, which seems to correspond to a small peak in Fig. 12. This peak is due again to a slight defect in the room temperature control.

If one admits that AE events are due to microcracking, these results show clearly that there is a coupling between creep and damage. It follows that the mechanical responses of beams subjected to creep compared to those not subjected to creep, ought to exhibit a difference due to initial damage accumulated during creep loads. A reduction of the residual carrying capacity due to basic creep has to be expected in particular.

3 RESIDUAL CAPACITY TESTS

In order to investigate the variation of the residual capacity due to creep, comparison specimens cast at the same time than those subjected to creep were kept under the same conditions of temperature and relative humidity. Three points bending experiments till failure were carried out on the creep loaded and on the comparison specimens.

The first series of test results deals with unotched beams under combined drying and basic creep. After 40 days of loading, beams of dimension D2 subjected to loads of 50% and 60% of the maximum load were removed from the creep frames and then immediately subjected to three point bending loading up to failure with a constant loading rate.

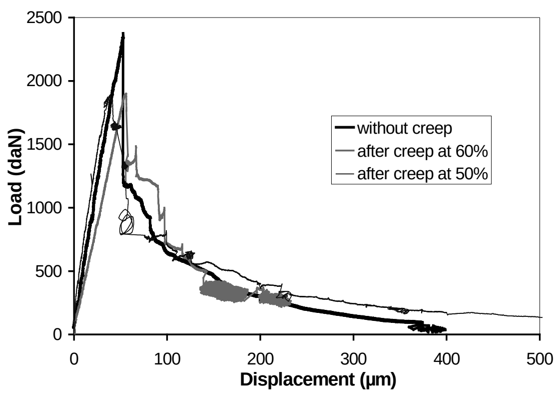

Figure 13. Residual capacity of unotched beams of dimension D2

The chosen rate of loading is 0,1µm/s, which is the same rate used as in the flexural experiments intended to determine the average maximum load for this kind of specimens (see section 2.2). Figure 13 displays the load-displacement curves obtained for the specimens after creep loading and for the unloaded comparison specimens. The maximum carrying force of the specimens subjected to creep initially is reduced of about 20% in comparison to those of the unloaded specimens. Furthermore, it is found that there is no significant impact of the loading level on the response of beams. The 50% and 60% loaded specimens have approximately the same peak load.

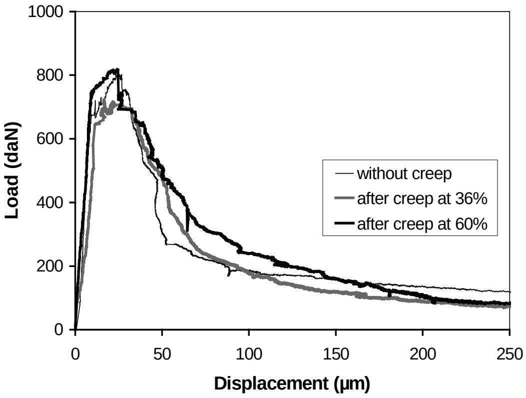

Figure 14. Residual capacity of notched beams of dimension D1

Figure 14 presents the results obtained on three points bend experiments carried out after 60 days of basic creep tests. These are notched specimens of dimension D1 loaded at 36% and 60% of the maximum load. Contrarily to previous results, it is observed that there is no influence of the 60 days of basic creep loading on the residual capacity of bending beams, when compared to the response obtained with the comparison specimens. The differences are within the experimental dispersion.

4 DISCUSSION AND CLOSURE

The following conclusions can be drawn from the above test results:

- For high load level, tertiary creep i.e. a visco-elastic response of the material coupled with an evolution of damage, occurs. In our bending tests, tertiary creep is observed for load levels that are above 60% of the maximum carrying capacity of the beam measured on initially unloaded specimens. This limit is consistent with other experimental data, namely on compression tests (Mazzotti and Savoia, 2003).

- Basic creep on bending beams seems to be size dependent. For two geometrically similar specimens (sizes D1 and D2), the displacement due to creep is neither equal nor multiplied by two (which is the ratio between the sizes of the two beams).

- AE shows that there is some activity during the creep phase. Such an activity should correspond to the development of microcracks. It is an indication that damage should be coupled to creep.

- Residual capacity tests show that drying creep has a great influence on the residual carrying capacity of the beams. For the tests presented, which are limited to low creep levels (50% and 60% of the maximum load), basic creep does not influence the structural strength of the beam.

These test results have now to be used for the development of a constitutive relation in which creep and damage are coupled. Some proposals exist in the literature (see for instance Mazzotti et al. 2001, Mazzotti and Savoia 2003, Zi and Bazant 2001, Bazant and Jirasek 1992, Omar et al. 2003, Benboudjema et al. 2001), and could be compared with the above results as well. Furthermore, additional test data dealing with larger sizes of specimen, higher load levels in basic creep experiments followed by size effect tests are expected to provide a more comprehensive understanding of the creep damage interaction and of the influence of creep on the fracture energy of concrete.

5 ACKNOWLEDGMENTS

Financial support from the European Commission through the MAECENAS project (FIS5-2001-00100) and from the partnership between Electricité de France and the R&DO group through the MECEN project are gratefully acknowledged.

6 REFERENCES

Bazant Z.P. 1988, Mathematical modeling of creep and shrinkage of concrete , John Wiley & Sons Ltd.

Bazant, Z.P. and Jirasek, M. 1992, R-curve modeling of rate effect in static fracture and its interference with size effect, in Fracture Mechanics of Concrete Structures. Proc. Int. Conf. On Fracture Mechanics of Concrete Structures. Breckenridge, Colorado, June, ed. by Bazant Z.P., Elsevier Applied Science, London, pp. 918-923.

Benboudjema F., Meftah F., Sellier A., Heinfling G. et Torrenti J.M. 2001, A basic creep model for concrete subjected to multiaxial loads, Fracture Mechanics of Concrete Structures, R. de Borst, J. Mazars, G. Pijaudier-Cabot and J.G.M. Van Mier Eds., Swets & Zeitlinger, Lisse, The Netherlands, pp. 161-168, 2001.

Berthelot J.M. and Robert J.L., 1987. Modelling concrete damage by acoustic emission. Journal of Acoustic Emission, 7, pp. 43 – 60.

Gettu, R., Bazant, Z.P. 1992, Rate effects and load relaxation: static fracture of concrete. ACI Materials J. 89 (5), pp. 456-468.

Granger L. Comportement différé du béton dans les enceintes de centrales nucléaires (analyse et modélisation) . Thèse de doctorat de l'ENPC, 1995.

Maji A.K. and Shah S.P., 1988. Process zone and acoustic emission in concrete. Experimental mechanics, 28, pp. 27 – 33.

Mazzotti C. and Savoia M., 2003, Nonlinear creep damage model for concrete under uniaxial compression, J. Engrg. Mech. ASCE, 129, pp. 1065-1075.

Mazzotti C., Savoia M., et Tralli A. 2001, An isotropic damage model for non linear creep behavior of concrete in compression, in Fracture Mechanics of Concrete Structures, R. de Borst, J. Mazars, G. Pijaudier-Cabot and J.G.M. Van Mier Eds., Swets & Zeitlinger, Lisse, The Netherlands, pp. 255-262.

Omar M., Pijaudier-Cabot G., and Loukili A. 2003, Etude du couplage endommagement – fissuration, Revue Française de Génie Civil, in press.

RILEM Draft Recommendations, 1990. Size effect method for determining fracture energy and process zone size of concrete, 23, pp. 461-465.

Rüsch H. 1957, Versuche zur Bestimmung des Einflusses der Zeit auf Festigkeit and Verformung, (Experimental Determination of the effect of the Duration of Loading on Strength and Deformation), *Final Report*, Fifth Congress, International Association for Bridge and Structural Engineering, Portugal, pp. 237-244.

Rüsch H., Sell R., Rasch C., Stöckl S. 1958, Investigations on the Strength of Concrete under Sustained Load, RILEM Symposium on the Influence of Time on the Strength and Deformation of concrete, Munich.

Zi G., Bazant Z.P. 2001, Continuous relaxation rpectrum of concrete creep and its incorporation incorporation into microplane model M4, Proc. CONCREEP-6, F.J. Ulm et al. Eds, Elsevier Pubs., pp. 239-243.